Structural and elastic properties of CaMg2 Laves phase by Y-parameter and Reuss-Voigt-Hill methods

Jia Fu[1 a], Jukui Guo[2], Hao Bai[1] and Weihui Lin[3]

[1]School of Materials Science and Engineering, Xi'an Shiyou University, Xi'an, 710065, China

[2]Xi'an Brake Branch, AVIC Aircraft Co., LTD., Xinping, 713106, China;

[3]International Center for Applied Mechanics, Xi'an Jiaotong University, Xi'an 710049, China.

*Corresponding author: [a] fujia@xsyu.edu.cn

Abstract. Structural, mechanical properties of CaMg2 Laves phase are investigated by the first-principle calculations and then the homogenized moduli are calculated by both the classical Reuss-Voigt-Hill estimation and a so-called Y parameter. Above all, the optimized crystal parameters are in very good agreement with the experimental data reported. Besides, elastic constants Cij are calculated, thus the shear modulus, bulk modulus, Young's modulus, Poisson's ratio are calculated to compare with the relative data in references. Contrary to Hill approach, the Y parameter enables to investigate the anisotropic characteristics and isotropic elastic properties of CaMg2 structure. By using Y parameter, we can see that Young's modulus and Poisson's ratio as a function of the compliance coefficient Sij (or elastic constants Cij) and plane orientation are distributed within a reasonable range, which are useful for the DFT study of similar hexagonal crystal structure at nanoscale.

1. Introduction

Magnesium (Mg) alloys cause more attention in recent years, as the best strength to weight ratio, low density and good stiffness [1, 2]. However, the practical application of magnesium alloys has not been widely used due to their restricted mechanical properties, as it easy to be oxidized as well as the limited mechanical properties [3,4]. Besides, by adding rare-earth (RE) elements, the mechanical properties of Mg-alloys can be greatly improved [5]. Besides, Ca can normally raise the density of aging precipitates $MgZn_2$ phase, therefore can improve the mechanical properties of the Mg-alloy [6]. Mg–Ca alloy has the combustion resistance and good oxidation [7]. The binary system of Mg-Ca has a good biocompatibility, no toxicity and appreciable corrosion resistance [8]. Zhang et al. [9] investigated the structural and thermodynamic properties of $CaMg_2$ in Mg–Al–Ca system. Ortegaet al. [10] investigated the precipitation process of $CaMg_2$ in Mg–Ca–(Zn) alloys by using positron annihilation spectroscopy. Zhong et al. [11] investigated the thermodynamic data of C14, C15 and C36 structures of $CaMg_2$. Moreover, as its excellent physical and chemical properties [12-14] in Mg-Ca, Mg-Al-Ca and Mg-Zn-Ca alloy systems, $CaMg_2$ Laves phase has caused more attention. Experimentally, some Laves phases $CaAL_2$ (C15), $CaMg_2$ (C14), $(Mg,Ca)Al_2$ (C14) and $Ca(Mg,Al)_2$ (C36) in Mg-Al-Ca alloys have been investigated [15,16]. Theoretically, Yu et al. [17] studied the mechanical properties of the AB_2-

type Laves, discovering that the $CaMg_2$ phase has a strong structural stability and the alloying ability. Tang et al. [3] investigated the elastic properties of $CaMg_2$ Laves phase, which suggests that $CaMg_2$ Laves phase has a strong stability. The stability and mechanical properties of the Mg-Ca system was studied by Zhou et al. [8], with the conclusion that $CaMg_2$ phase is ductile. Mao et al. [18] investigated the mechanical properties of intermetallics in the Mg-Zn-Ca-Cu alloy. However, there is no theoretical systematically study reported about the structural, mechanical properties of $CaMg_2$ phase. Elastic moduli of polycrystals can be calculated by Y-parameter and the Reuss-Voigt-Hill (RVH) methods [20-24]. Musgrave [25] and Neighbours [26] have discussed the propagation velocities of sound for different crystal symmetrys.

In this work, the Y-parameter and Reuss-Voigt-Hill (RVH) methods are used to investigate elastic properties of the $CaMg_2$ phase. Hence, this work aim to study about the elastic properties of C14-type $CaMg_2$ phase on the basis that Young's modulus is the function of the elastic constants in a certain orientation of the crystal plane. These are useful for similar hexagonal structure with the same space group P63/mmc at nanoscale.

2. Modelling and computational method

2.1 Modelling of CaMg2 crystal

Manganese carbonate crystals belong to the hexagonal type, the space group is P63/mmc type, and the lattice parameters are as follows: $a=b=6.25$Å, $c=10.10$Å, $\alpha=\beta=90°$, $\gamma=120°$. Its crystal structure is in Figure 1.

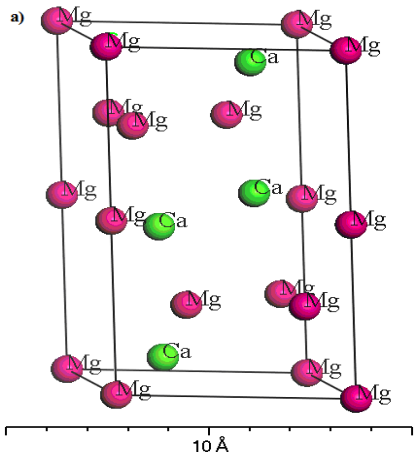

Figure 1. Schematic diagram of $CaMg_2$ crystal structure.

As in Figure 1, Mg atoms are located on *2a*, *6f* sites. Besides, Ca atoms are located on *4f* sites. For Mg *2p6 3s2* and Ca *3s2 3p6 4s2*, the Pseudo atomic calculations are carried out. The lattice parameters are optimized for energy minimization.

2.2 computational method

CASTEP as an first-principles plane wave pseudo-potential method is used for the calculations. The exchange correlation potential is considered by the generalized gradient approximation (GGA). The cut-off energy of the plane wave is set as 400eV to fully converge during calculation. The Brillouin zone with a mesh of 12×12×8 is generated by Monkhorst-Pack method. Geometry optimization is carried out with optimizing cell by the scheme of the Brodyden - Fletcher - Goldfarb - Shanno (BFGS) minimization until the total energy convergence value is 5.0×10^{-6} eV/atom, the pressure region is 0～60*GPa*.

3 Result analysis and discussion

3.1 Lattice parameters and elastic constants

3.1.1 Lattice parameters

The lattice parameters at 0MPa are shown in Table 1.

Table 1. Lattice *a*, *b*, *c* (Å) of $CaMg_2$ crystal.

	a_0(Å)	c_0(Å)	c_0/a_0	V_0(Å^3)
This work	6.250	10.101	1.616	341.732
Cal. [3]	6.232	10.093	1.620	339.740
Exp. [16]	6.220	10.100	1.624	341.081
Cal. [17]	6.240	10.140	1.625	342.200

From Table 1, the c/a ratio used is 1.616, within the relative error range of the experiment, which match better to Tang [3] 1.620, Aono [16] 1.624 and Yu [17] 1.625.

3.1.2 Elastic constants

Elastic constants C_{ij} (GPa) of $CaMg_2$ crystal is in Table 2.

Table 2. Elastic constants C_{ij} of $CaMg_2$ crystal.

	C_{11}	C_{12}	C_{13}	C_{33}	C_{44}
This work	55.70	18.05	15.26	58.39	16.95
Cal. [5]	62.95	15.27	13.64	65.20	17.77
Cal. [18]	51.43	22.31	14.73	58.51	14.32
Exp. [27]	56.25	15.90	15.00	61.63	18.05

From Table 2, we can see that C_{33} is the largest, indicating that the stiffness in this direction is the largest. C_{33} in *c*-axis direction is perpendicular to the atomic plane composed of *a*-axis and *b*-axis. Elastic constants C_{ij} under various pressures of 0-60GPa is in Figure 2.

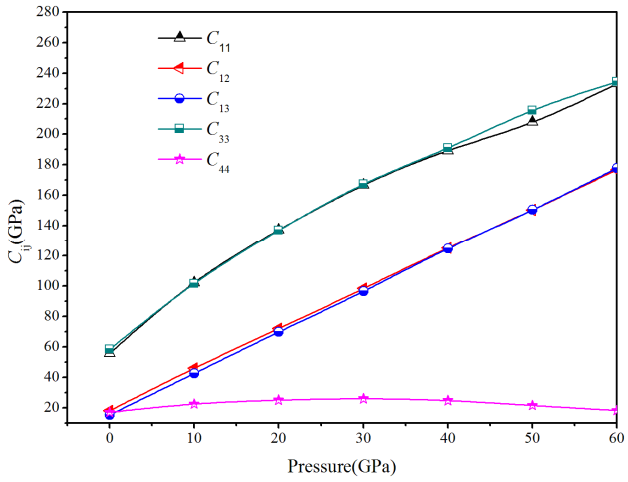

Figure 2. Elastic constants under pressure of 0- 60GPa

From Figure 2, the variation of elastic constants under different pressures is not the same, where the slope of the C_{11} and C_{33} change curves is positive. The contribution of C_{33} to elasticity is greater

than that of the *a*-axis C_{11} and the *b*-axis C_{22}. The rest elastic constants slightly increased but tended to be relatively steady.

3.2 Reuss bound and Voigt bound

3.2.1 Reuss bound and Voigt bound

For hexagonal crystals[21], the elastic constants should satisfy the generalized stability criteria. Generally, the Reuss and Voigt bounds of hexagonal crystals are as [21]:

$$C_{11}>0; C_{11}-C_{12}>0; C_{44}>0; (C_{11}+C_{12})C_{33}-2C_{13}^2>0 \quad (1)$$

$$G_V=\frac{1}{30}(7C_{11}-5C_{12}+12C_{44}+2C_{33}-4C_{13}) \quad (2)$$

$$G_R=\frac{5}{2}\left\{\frac{[(C_{11}+C_{12})C_{33}-2C_{13}^2]C_{44}C_{66}}{3B_VC_{44}C_{66}+[(C_{11}+C_{12})C_{33}-2C_{13}^2](C_{44}+C_{66})}\right\} \quad (3)$$

$$B_V=\frac{2}{9}(C_{11}+C_{12}+\frac{1}{2}C_{33}+2C_{13}) \quad (4)$$

$$B_R=\frac{(C_{11}+C_{12})C_{33}-2C_{13}^2}{C_{11}+C_{12}+2C_{33}-4C_{13}} \quad (5)$$

Based on the upper boundary (Voigt bound) and lower boundary (Reuss bound), elastic moduli can be calculated [21,23] as follows: G_v=18.63*GPa*, B_v=29.66*GPa*, G_r=18.48*GPa*, B_r=29.65*GPa*, *B*=25.66*GPa*, *G*=18.55*GPa*, *E*=46.05*GPa*, μ=0.241. Besides, values of the B (29.66GPa) and G (18.55GPa) are consistent with the values of 29.43GPa and 15.72GPa by the experimental measurement of Mao [18].

3.2.2 The compliance coefficient

Elastic constant characterizes the response of the lattice to external stress within the elastic limit [8]. For hexagonal crystal, the interchangeable relation between C_{ij} and S_{ij} are as follows [28]:

$$S_{11}=\frac{C_{33}}{2C_{33}(C_{11}+C_{12})-2C_{13}^2}+\frac{1}{2(C_{11}-C_{12})} \quad (6)$$

$$S_{12}=\frac{C_{33}}{2C_{33}(C_{11}+C_{12})-2C_{13}^2}-\frac{1}{2(C_{11}-C_{12})} \quad (7)$$

$$S_{13}=-\frac{C_{13}}{C_{33}(C_{11}+C_{12})-2C_{13}^2} \quad (8)$$

$$S_{33}=\frac{C_{11}+C_{12}}{C_{33}(C_{11}+C_{12})-2C_{13}^2} \quad (9)$$

$$S_{44}=C_{44}^{-1} \quad (10)$$

Young's modulus describes the linear deformation behaviors of the crystal, its value in three directions of *a*, *b*, and *c* axes can be obtained from the inverse S_{ij} matrix in Cartesian coordinates: $E_x = S_{11}^{-1}$, $E_y = S_{22}^{-1}$, And $E_z = S_{33}^{-1}$. The S_{ij} can be obtained by inverse matrix.

Thus, the compliance coefficient S_{ij} can be calculated as: S_{11}=0.0209, S_{33}=0.0590, S_{12}=-0.0057, S_{13}=-0.0040. By the definition, thus: E_x=E_y=47.8469GPa, E_z=16.9492GPa.

3.2.3 Y-parameter expressions

Based on the Reuss bound, *Y* parameter including elastic modulus E_Y and Shear modulus G_Y of the hexagonal crystal surface normal (n=(u, v, w)) are as [29]:

$$E_Y(u,v,w)=1\Big/\left\{S_{11}-\left[2(S_{11}-S_{13})-S_{44}\right]w^2+(S_{11}-2S_{13}+S_{33}-S_{44})w^4\right\} \quad (11)$$

$$G_Y(u,v,w) = 1/\{(2S_{11} - S_{12} - S_{13}) - (5S_{11} - S_{12} - 5S_{13} + S_{33} - 3S_{44})w^2 + 3(S_{11} - 2S_{13} + S_{33} - S_{44})w^4 \quad (12)$$

Where w is a normal direction cosine of hexagonal crystal surface.

Similarly, for Voigt bound, E_Y and G_Y are as [29]:

$$E_Y(u,v,w) = [2C_{11} - C_{12} - C_{13} - w^2(5C_{11} - C_{12} - 5C_{13} + C_{33} - 12C_{44}) + 3w^4(C_{11} - 2C_{13} + C_{33} - 4C_{44})] \cdot [C_{11} + C_{12} + C_{13} - w^2(C_{11} + C_{12} - C_{13} - C_{33})] / [2C_{11} + C_{12} + C_{13} - w^2(3C_{11} + C_{12} - 3C_{13} - C_{33} - 4C_{44}) + w^4(C_{11} - 2C_{13} + C_{33} - 4C_{44})] \quad (13)$$

$$G_Y(u,v,w) = \frac{1}{4}[2C_{11} - C_{12} - C_{13} - w^2(5C_{11} - C_{12} - 5C_{13} + C_{33} - 12C_{44}) + 3w^4(C_{11} - 2C_{13} + C_{33} - 4C_{44})] \quad (14)$$

When w^2=1/3, Young's modulus is equal to the calculation result by Hill model.

Relations between compliance coefficient S_{ij} and Young's modulus E_Φ (or shear modulus G_Φ) in either direction of hexagonal crystal making an angle Φ with c-axis are [28]:

$$\frac{1}{E_\phi} = S_{11}(1 - l_3^2)^2 + S_{33}l_3^4 + (2S_{13} + S_{44})l_3^2(1 - l_3^2) \quad (15)$$

$$\frac{1}{G_\phi} = S_{44} + \left(S_{11} - S_{12} - \frac{S_{44}}{2}\right)(1 - l_3^2) + 2(S_{11} + S_{33} - 2S_{13} - S_{44})l_3^2(1 - l_3)^2 \quad (16)$$

Where, $l_3 = \cos\theta$ is the cosine of normal orientation L_3 within crystal plane of hexagonal crystal.

3.3 Elastic moduli by various methods

3.3.1 Homogenized elastic moduli by RVH

Based on calculated C_{ij}, homogenized moduli are obtained by RVH method. Voigt and Reuss approximations showing upper limit and lower limit are in Table 3, the difference within acceptable errors arises due to the use of different parameter C_{ij} in calculation.

Table 3. Mechanical moduli (unit: *GPa*) of $CaMg_2$ crystalline by various methods

	B_v	B_r	G_v	G_r	B	G
This work	29.66	29.65	18.63	18.48	29.66	18.55
Cal. [5]	30.69	30.69	21.78	21.24	30.69	21.51
Cal. [18]	29.43	29.43	15.95	15.50	29.43	15.72
Exp. [27]	29.55	29.51	19.80	19.66	29.53	19.73

From Table 3, we can see that elastic moduli by Y-parameter are consistent with the classical Reuss-Voigt-Hill (RVH) calculation. The relation G=E/[2(1+ν)] are satisfied with parameters in Table 3 and Table 4.

3.3.2 Surface of elastic modulus

The universal anisotropic index (A_U), the percentage of anisotropy in compression and shear (A_B and A_G) are [30]:

$$A^U = 5\frac{G_V}{G_R} + \frac{B_V}{B_R} - 5 \ , \ A_G = \frac{G_V - G_R}{G_V + G_R} \times 100\% \quad (17)$$

Where the B_V, B_R, G_V and G_R refers to the Voigt and Reuss approximations of bulk modulus and shear modulus. A^U=0 corresponds to isotropic structure. A_G=1 stands for the largest elastic anisotropy . Young's modulus E, Poisson's ratio ν, bulk to shear modulus ratio B/G, and elastic anisotropy indexes (A^U and A_G) are listed in Table 5.

Table 4. Young's modulus E, Poisson's ratio ν, bulk to shear modulus ratio B/G, and elastic anisotropy indexes (A^U and A_G).

	ν	A^U	A_G	B/G	*E* (*GPa*)
This work	0.241	0.040	0.004	1.598	46.055
Cal. [5]	0.216	0.127	0.013	1.427	52.309
Cal. [18]	0.273	0.143	0.014	1.872	40.043
Exp.[27]	0.227	0.037	0.004	1.497	48.415

Surface of elastic modulus by DFT calculation of $CaMg_2$ compound is shown in Fig.4.

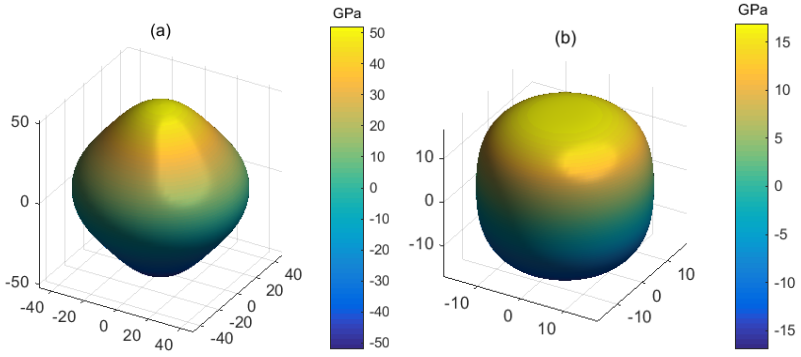

a)Young's modulus; b)Shear modulus;

Figure 3. Surface of elastic modulus by DFT calculation of $CaMg_2$ crystal

From Figure 3, Young's modulus and shear modulus are anisotropic, showing a certain anisotropy. Young's modulus *E* of $CaMg_2$ compound is 46.055 GPa, which demonstrates manganese carbonate is a relatively stiffer material. Poisson ratio is 0.241, which is close to other references[5, 18, 27].

3.3.3 Elastic moduli variation by Y-parameter

Young's and Poisson ratio of $CaMg_2$ structure by Y-parameter are in Figure 4.

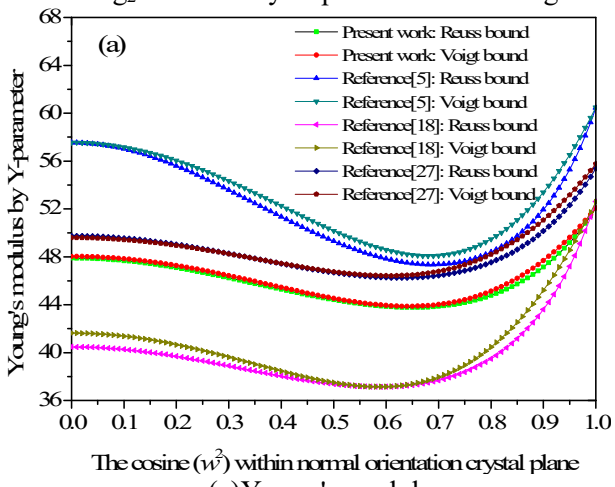

(a)Young's modulus;

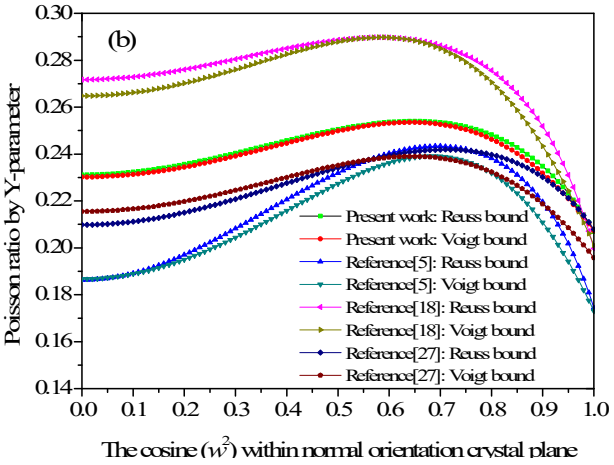

(b) Shear modulus

Figure 4. Young's modulus and Poisson ratio of $CaMg_2$ by the Y parameter

As from Fig.4 a) -Fig.4 b), Young's modulus and Poisson's ratio of $CaMg_2$ are closed to each other. Moreover, Young's modulus E is between 43.77*GPa* and 52.07*GPa,* Poisson ratio v is between 0.207 and 0.254. Elastic moduli of $CaMg_2$ compound based on C_{ij} can be calculated by RVH estimation[21-24]. It can be seen that, when w^2=1/3, values of E and v are 46.05GPa and 0.24, which are equal to results of Hill model.

4. Conclusion

Generally, elastic properties of $CaMg_2$ crystal is investigated and C_{ij} determination are given by DFT method. Y-parameters have then been determined for $CaMg_2$ crystal structures in the homogenization of elastic properties. Results are as follows:

(1) The calculated lattice parameters (a, b and c), the independent elastic constants, mechanical properties and the elastic anisotropy factor A are in very good agreement with the experimental literatures.

(2) The G/B ratio of shear modulus to bulk modulus at 0GPa is 0.663, which indicates slight brittleness of $CaMg_2$ phase at zero pressure.

(3) For Y parameter, when w^2=1/3, E is 46.05GPa, which is equal to the result of Hill model. Therefore, using Y parameter method to study elastic moduli of $CaMg_2$ phase is quietly feasible.

Acknowledgement

The authors acknowledge the financial support by national science foundation of China (NSFC) (No.51174140, 21671096, 51275414) and the support of start-up foundation of Xi'an Shiyou University. Thanks to Qiufeng Wang for her personnel support.

References

[1] C. Potzies, K.U. Kainer, Advanced Engineering Materials, **6**, 281-289 (2004).
[2] Z.B. Sajuri, T. Umehara,Y. Miyashita et al., Advanced engineering materials, **5**, 910-916 (2003).
[3] B.Y. Tang, W.Y.Yu, X.Q. Zeng et al., Materials Science and Engineering: A, **489**, 444-450 (2008).
[4] J.F. Nie, Scripta Mater. **48** (2003) 981.
[5] B.L. Mordike, T. Ebert, Materials Science and Engineering: A, **302**, 37-45 (2001).
[6] K. Oh-Ishi, C.L. Mendis, T. Homma, S. Kamado et al., Acta Materialia, **57**, 5593-5604 (2009).
[7] J.F. Fan, G.C. Yang, H. Xie, W.X. Hao, M. Wang, G.C. Yang, Y.H. Zhou, Mater. Trans. A **361** (2005) 235.
[8] P. Zhou and H. R. Gong, Journal of the mechanical behavior of biomedical materials, **8**, 154-164 (2012).
[9] H. Zhang, S.L. Shang, Y. Wang, L.Q. Chen, Z.K. Liu, Intermetallics, **22** (2012) 17.

[10] Y. Ortega, M.A. Monge, R. Pareja, J. Alloys Compd., **463** (2008) 62.
[11] Y. Zhong, K. Qzturk, J.O. Sofo, Z.K. Liu, J. Alloys Compd. **420** (2006) 98.
[12] G. Yuan, Y. Liu, W. Ding, et al., Materials Science and Engineering: A, **474**, 348-354 (2008).
[13] Y. Liu, G. Yuan, W. Ding, et al., Journal of alloys and compounds, **427**, 160-165 (2007).
[14] W. Chen, J.Sun, Physica B: Condensed Matter, **382**, 279-284 (2006).
[15] P. Zhou and H. R. Gong, Journal of the mechanical behavior of biomedical materials, **8**, 154-164 (2012).
[16] K. Aono, S. Orimo, and H. Fujii., Journal of alloys and compounds, **309**, L1-L4 (2000).
[17] W.Y. Yu, N. Wang, X.B. Xiao, B.Y. Tang et al., Solid State Sciences, **11**, 1400-1407 (2009).
[18] Mao P, Yu B, Liu Z, et al., Journal of Magnesium and Alloys, **1**, 256-262 (2013).
[19] Jia Fu, Fabrice Bernard, Siham Kamali-Bernard, Molecular Simulation, **44**(4), 285-299 (2018).
[20] Jia Fu, K.-B. Siham, B. Fabrice, Marilyne Cornen, Compos Part B-Eng, **150**, 1-15 (2018).
[21] Jia Fu, B. Fabrice, K.-B. Siham, J Phys Chem Solids,**101**,74-89 (2017).
[22] Jia Fu, B. Fabrice, K.-B. Siham, J Nano Res. **33**, 92-105 (2015).
[23] Jia Fu, Weihui Lin, Zhongren Chen. IJAMP,**1**(1), 62-69 (2016).
[24] Jia Fu,Weihui Lin, AER, **120**, 390-395 (2017).
[25] M. J. P. Musgrave, Proc. Roy. Soc. (London) A226, **339**(1954).
[26] J. R. Neighbours, J. Acoust. Soc. Am. 26, **865** (1954).
[27] Ali Sumer and J. F. Smith, Journal of Applied Physics **33**, 2283 (1962).
[28] D.Raabe, *Wiley-VCH*,Weinheim,1998.
[29] Zheng, L., Min, L., Acta Physica Sinica, **58**(12), 8511-8521 (2009).
[30] B. Xiao, J. Feng, C. T. Zhou, Y. H. Jiang and R. Zhou, J. Appl. Phys., **109**, 023507 (2011).